

Sample genealogies and genetic variation in populations of variable size

A. Eriksson^{a,b}, B. Mehlig^a, M. Rafajlovic^a, and S. Sagitov^c

^a *Department of Physics, University of Gothenburg, SE-41296 Gothenburg, Sweden*

^b *Department of Zoology, University of Cambridge, Cambridge, UK*

^c *Mathematical Sciences, Chalmers University of Technology and University of Gothenburg, SE-41296 Gothenburg, Sweden*

We consider neutral evolution of a large population subject to changes in its population size. For a population with a time-variable carrying capacity we have computed the distributions of the total branch lengths of its sample genealogies. Within the coalescent approximation we have obtained a general expression – Eq. (27) – for the moments of these distributions for an arbitrary smooth dependence of the population size on time. We investigate how the frequency of population-size variations alters the distributions. This allows us to discuss their influence on the distribution of the number of mutations, and on the population homozygosity in populations with variable size.

Keywords: Population-size fluctuations, population homozygosity, genealogy, single-nucleotide polymorphisms, coalescent approximation

I. INTRODUCTION

Models for gene genealogies of biological populations often assume a constant, time-independent population size N . This is the case for the Wright-Fisher model (FISHER, 1930; WRIGHT, 1931), for the Moran model (MORAN, 1958), and for their representation in terms of the coalescent (KINGMAN, 1982). In real biological populations, by contrast, the population size changes over time. Such fluctuations may be due to catastrophic events (bottlenecks) and subsequent population expansions, or just reflect the randomness in the factors determining the population dynamics. Many authors have argued that genetic variation in a population subject to size fluctuations may nevertheless be described by the Wright-Fisher model, if one replaces the constant population size in this model by an effective population size of the form

$$N_{\text{eff}} = \left(\lim_{T \rightarrow \infty} \frac{1}{T} \int_0^T \frac{dt}{N(t)} \right)^{-1} \quad (1)$$

(see, e.g., EWENS (1982) for a review of different measures of the effective population size, and SJÖDIN *et al.* (2005); WAKELEY and SARGSYAN (2009) for recent extensions of this concept). The harmonic average in Eq. (1) is argued to capture the significant effect of catastrophic events on patterns of genetic variation in a population: if for example a population went through a recent bottleneck, a large fraction of individuals in a given sample would originate from few parents. This in turn would lead to significantly reduced genetic variation, parameterised by a small value of N_{eff} .

The concept of an effective population size has been frequently used in the literature, implicitly assuming that the distribution of neutral mutations in a large population of fluctuating size is identical to the distribution in a Wright-Fisher model with the corresponding constant effective population size given by Eq. (1). However, recently it has been shown that this is true only under certain circumstances (JAGERS and SAGITOV, 2004; KAJ and KRONE, 2003; NORDBORG and KRONE, 2003). It is argued by SJÖDIN *et al.* (2005) that the concept of an effective population size is appropriate when the time scale of fluctuations of $N(t)$ is either much smaller or much larger than the typical time between coalescent events in the sample genealogy. In these limits it can be proven that the distribution of the sample genealogies is exactly given by that of the coalescent with a constant, effective population size.

More importantly, it follows from these results that, in populations with variable size, the coalescent with a constant effective population size is not always a valid approximation for the sample genealogies. Deviations between the predictions of the standard coalescent model and empirical data are frequently observed, and there is a number of different statistical tests quantifying the corresponding discrepancies (see for example (FU and LI, 1993; TAJIMA, 1989; ZENG *et al.*, 2006)). The analysis of such deviations is of crucial importance in understanding for example human genetic history (GARRIGAN and HAMMER, 2006). But while there is a substantial amount of work numerically quantifying deviations, often in terms of a single number, little is known about their qualitative origins and their effect upon summary statistics in the population in question.

The aim of this paper is to study the effect of population-size fluctuations on the patterns of genetic variation for the case where the scale of the population-size fluctuations is comparable to the time between coalescent events in the ancestral tree. As is well-known, empirical measures of genetic variation can usually be computed from the total branch length of the sample genealogy (the expected number of single-nucleotide polymorphisms, for example, is proportional to the average total branch length). In the following we therefore analyse the distributions of the total branch lengths for sample genealogies in a population of fluctuating size. An example is given in Fig. 1 which shows numerically computed branch-length distributions for a particular model population (described in Sec. IV) with a time-dependent carrying capacity.

As Fig. 1 shows, the distributions depend in a complex manner on the form of the size changes. We observe that when the frequency of the population-size fluctuations is either very small or very large, the results are well described by Kingman's coalescent with a constant (effective) population size. Apart from these special limits, however, the form of the distributions appears to depend in a complicated manner upon the frequency of the population-size variation. The observed behaviour is caused by the fact that coalescence proceeds faster for smaller population sizes, and more slowly for larger population sizes, as illustrated in Fig. 2. But the question is how to quantitatively account for the changes displayed in Fig. 1.

We show in this paper that the results of the simulations shown in Fig. 1 are explained by a general expression – Eq. (27) – for the moments of the distributions shown in Fig. 1. Our general result is obtained within the coalescent approximation valid in the limit of large population size. But we find that in most cases, the coalescent approximation works very well down to small population sizes (a few hundreds of individuals). Our result enables us to understand and quantitatively describe the frequency dependencies of the distributions shown in Fig. 1. It makes possible to determine for example how the variance, skewness, and the kurtosis of these distributions depend upon the frequency of demographic fluctuations. This in turn allows us to compute the population homozygosity and to characterise genetic variation in populations with size fluctuations.

The remainder of this paper is organised as follows. In Sec. II we review how empirical observables are related to the branch lengths of the sample genealogies. Section III summarises our analytical results for the moments of the total branch length. In Sec. IV we describe the model employed in the computer simulations. The corresponding numerical results are compared to the analytical predictions in Sec. V. Finally, in Sec. VI we summarise how population-size fluctuations influence the distribution of total branch lengths, discuss the implications for patterns of genetic variation, and conclude with an outlook.

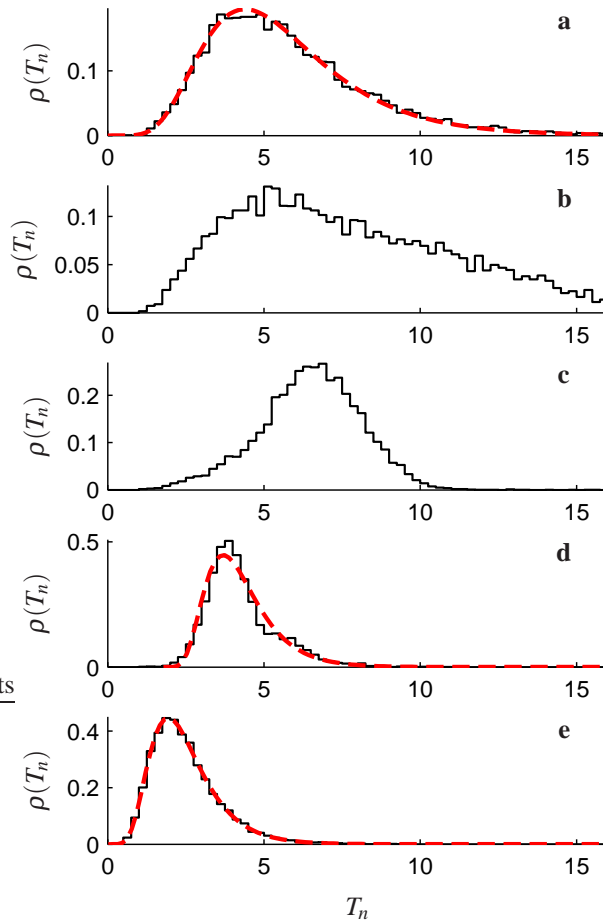


FIG. 1 Numerically computed distributions $\rho(T_n)$ of total branch lengths T_n in genealogies of samples of size $n = 10$. The model employed in the simulations is outlined in Sec. IV. It describes a population subject to a time-varying carrying capacity. Panels **a** to **e** show $\rho(T_n)$ for populations with increasingly rapidly oscillating carrying capacity. The dashed red line in **a** shows a low-frequency approximation to $\rho(T_n)$ obtained for a constant carrying capacity. The dashed red lines in **d** and **e** show the large-frequency approximations given by Eq. (49). Further numerical and analytical results on the frequency dependence of the moments of these distributions are shown in Fig. 5. Parameter values (see Sec. IV for details): $K_0 = 10,000$, $r = 1$, $\varepsilon = 0.9$, and **a** $\nu K_0 = 0.001$, **b** $\nu K_0 = 0.1$, **c** $\nu K_0 = 0.316$, **d** $\nu K_0 = 1$, and **e** $\nu K_0 = 100$.

II. OBSERVABLES

In this section we review how empirical observables are related to the branch lengths of the sample genealogies.

Patterns of genetic variation reflect the gene genealogy corresponding to a given sample. Within a neutral infinite-sites model, mutations are assumed to occur randomly at a constant rate μ on the genealogy. For a sample of size n , the number S_n of single-nucleotide polymorphisms conditioned on the total branch length T_n of the sample genealogy has a Poisson distribution with mean $\theta T_n/2$ (here θ is a scaled mutation parameter, $\theta = 2\mu N_0$ where N_0 is a suitable measure of the population size):

$$\langle S_n \rangle = \frac{\theta}{2} \langle T_n \rangle. \quad (2)$$

Similarly, moments of S_n can be computed in terms of moments of T_n . As is well known, the corresponding relations are most conveniently expressed in terms of the function $F_n(q)$ from which the moments can be computed by repeated differentiation with respect to q :

$$F_n(q) = \langle e^{-qT_n} \rangle, \quad \text{so that} \quad \langle T_n^k \rangle = (-1)^k \frac{d^k}{dq^k} F_n(0). \quad (3)$$

Note that $F_n(\theta/2)$ is the probability of observing no mutations in a sample of size n (thus $F_2(\theta/2)$ is the population homozygosity).

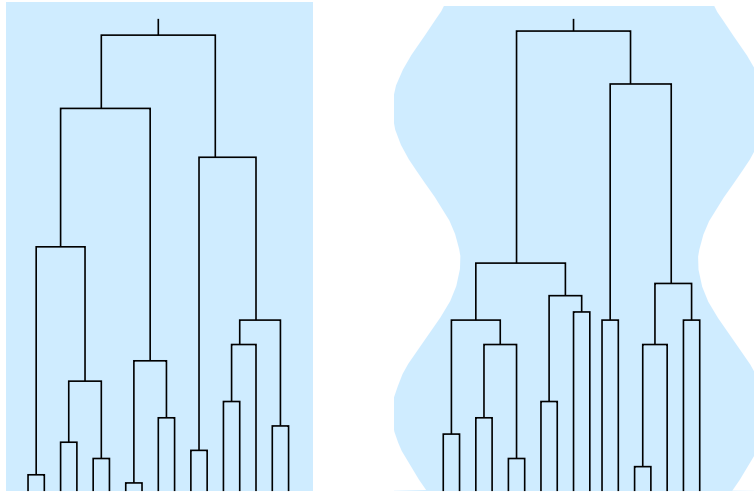


FIG. 2 Illustrates the effect of population-size oscillations on the genealogy of a sample of size $n = 17$ (schematic). Left: genealogy described by Kingman's coalescent for a large population of constant size, illustrated by the light blue rectangle. Right: sinusoidally varying population size. Coalescence is accelerated in regions of small population sizes, and vice versa. This significantly alters the tree and gives rise to changes in the distribution of the number of mutations, and of the population homozygosity.

The corresponding function for the moments of S_n is found to be:

$$\langle e^{-qS_n} \rangle = F_n \left(\frac{\theta}{2} (1 - e^{-q}) \right). \quad (4)$$

For a constant population size, this equation is equivalent to Eq. (1.3a) in (WATTERSON, 1975).

In short, the distribution of single-nucleotide polymorphisms is determined by the function $F_n(q)$, or equivalently by the moments $\langle T_n^k \rangle$.

Microsatellite loci by contrast are usually modeled in terms of a step-wise mutation model (OHTA and KIMURA, 1973) in which a mutation corresponds to either the gain or, equally likely, the loss of a repeat unit. Provided that such steps (mutations) occur according to a Poisson process, the distribution of the difference j in the numbers of repeats between two randomly sampled sequences is determined by the function F_2 (KIMMEL and CHAKRABORTY, 1996; OHTA and KIMURA, 1973):

$$p_j = \frac{1}{2\pi} \int_0^{2\pi} d\omega \cos(\omega j) F_2(\theta(1 - \cos \omega)). \quad (5)$$

In summary, the function F_n (or equivalently the moments $\langle T_n^k \rangle$) allow to compute the statistical fluctuations of the numbers of single-nucleotide polymorphisms and of the number of steps in a step-wise mutation model. In Sec. III we show how the moments and the function $F_n(q)$ may be determined for a large neutral population subject to smooth population-size changes of otherwise arbitrary form.

III. COALESCENT APPROXIMATION FORMULAE FOR $F_n(q)$ AND $\langle T_n^k \rangle$

In this section we show how to calculate the function $F_n(q)$ and the moments $\langle T_n^k \rangle$ within the coalescent approximation, for a population with a smoothly varying size.

For $q = \theta/2$, the quantity $F_{n-1}(\theta/2)$ is just the probability that $n - 1$ sequences sampled at the present time are identical. Thus in a population of constant size, $F_n(q)$ is given by

$$F_n(q) = \frac{\binom{n}{2}}{\binom{n}{2} + nq} F_{n-1}(q). \quad (6)$$

This recursion has the well-known solution (with initial condition $F_1 = 1$)

$$F_n(q) = \frac{\Gamma(n)\Gamma(1+2q)}{\Gamma(n+2q)}. \quad (7)$$

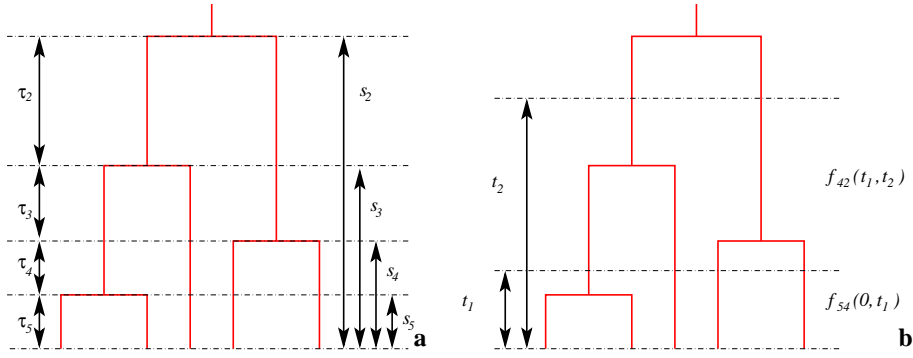


FIG. 3 **a** Illustrates the definition of the variables τ_j and $s_j = \sum_{k=j}^n \tau_k$ used in the calculation of $F_n(q)$. In the example given, the sample size is $n = 5$. **b** Illustrates the definition of the times in Eq. (21).

The question is how to obtain a corresponding expression for the case of a changing population size. We assume that in the limit of large population sizes, the changes in population size are described by a smooth curve $x(t) = N(t)/N_0$, so that $0 < x(t) \leq 1$ and $x(0) = x_0$ at the present time, $t = 0$. As common in the coalescent approximation time is counted ‘backwards’, that is t increases from the present ($t = 0$) to the past.

Given a realisation of the curve $x(t)$, the function $F_n(q)$ can be calculated as follows. The starting point is the joint distribution of times τ_j (illustrated in Fig. 3a). As shown by GRIFFITHS and TAVARÉ (1994) it can be written in terms the variables $s_j = \sum_{k=j}^n \tau_k$:

$$f(\tau_2, \dots, \tau_n) = \prod_{j=2}^n b_j x(s_j)^{-1} e^{-b_j[\Lambda(s_j) - \Lambda(s_{j+1})]}. \quad (8)$$

Here $b_j = j(j-1)/2$ and $\Lambda(t) = \int_0^t dt' x(t')^{-1}$ is the ‘population-size intensity function’ defined by GRIFFITHS and TAVARÉ (1994). The distribution of the times τ_j during which the sample genealogy has j lines depends upon the sample size n . This dependence is not made explicit here, neither in Eq. (8) nor in the following. The corresponding joint density for the variables s_j is simply (TAVARÉ, 2004)

$$g(s_2, \dots, s_n) = \prod_{j=2}^n b_j x(s_j)^{-1} e^{-b_j[\Lambda(s_j) - \Lambda(s_{j+1})]} \quad (9)$$

(for $0 < s_n < s_{n-1} < \dots < s_2$, and $s_{n+1} = 0$).

Now we make use of the fact that the total time is given by

$$T_n = s_n + s_{n-1} + \dots + s_3 + 2s_2. \quad (10)$$

(see Fig. 3a). The function $F_n(q)$ can therefore be written as

$$F_n(q) = \int_{0 < s_n < s_{n-1} < \dots < s_2} ds_n \dots ds_2 g(s_2, \dots, s_n) e^{-q(s_n + s_{n-1} + \dots + s_3 + 2s_2)}. \quad (11)$$

Expanding the multiple integrals one obtains

$$F_n(q) = b_n \int_0^\infty \frac{ds_n}{x(s_n)} e^{-[(n-1)\Lambda(s_n) + qs_n]} \dots b_2 \int_{s_3}^\infty \frac{ds_2}{x(s_2)} e^{-[\Lambda(s_2) + 2qs_2]}. \quad (12)$$

For small sample sizes n , Eq. (12) provides a convenient way of computing the function $F_n(q)$ and the corresponding moments $\langle T_n^k \rangle$. For example, for $n = 2$ one finds simply

$$F_2(q) = 1 - 2q \int_0^\infty dt e^{-\Lambda(t) - 2qt}, \quad (13)$$

$$\langle T_2^k \rangle = 2^k k \int_0^\infty dt t^{k-1} e^{-\Lambda(t)}. \quad (14)$$

This makes it possible to compute the population homozygosity in large populations with arbitrary size variations, as well as the

distribution of steps in a step-wise mutation model, according to Eq. (5).

For large values of n , by contrast, the large number of nested integrals in (12) becomes increasingly difficult to evaluate. In this limit, however, the distribution is conveniently characterised in terms of its cumulants which can be expressed in terms of the moments $\langle T_n^k \rangle$.

In the remainder of this section we show how to calculate the moments for arbitrary sample sizes n . According to Eq. (3), these moments are obtained by repeated differentiation of Eq. (12). However, in the following we describe a more elegant approach making use of a result obtained by TAVARÉ (1984). As Fig. 3a shows, an alternative expression for the total time is simply $T_n = \sum_{m=2}^n m \tau_m$. The k -th moment of the distribution of T_n is therefore

$$\langle T_n^k \rangle = \sum_{\substack{v_2, v_3, \dots, v_n \\ v_2 + v_3 + \dots + v_n = k}} \binom{k}{v_2, v_3, \dots, v_n} n^{v_n} \dots 2^{v_2} \langle \tau_n^{v_n} \dots \tau_2^{v_2} \rangle \quad (15)$$

where the variables v_j can assume values between 0 and k (subject to the constraint $v_2 + v_3 + \dots + v_n = k$). In a population of constant size, $x = 1$, the variables τ_j are independent and their correlation functions factorise. In general this is not the case: ZIVKOVIC and WIEHE (2008), for example, have calculated $\langle \tau_i \tau_j \rangle$ for a smoothly varying population (Eqs. (2) and (3) in their paper).

In the following we show how the correlation functions of arbitrary order appearing in (15) can be calculated in a very simple manner. Consider first the case $k = 1$. We have

$$\tau_j = \int_0^\infty dt \mathbf{1}_{\{\ell(t)=j\}}. \quad (16)$$

Here $\ell(t)$ denotes the number of lines for a particular realisation of the coalescent process at time t in a sample of size $n = \ell(0)$. The indicator function in Eq. (16) is unity when $\ell(t) = j$ and zero otherwise. Averaging over realisations gives

$$\langle \tau_j \rangle = \int_0^\infty dt \langle \mathbf{1}_{\{\ell(t)=j\}} \rangle = \int_0^\infty dt f_{nj}(0, t). \quad (17)$$

Here $f_{nm}(t_1, t_2)$ is the conditional probability that n ancestral lines at t_1 coalesce to m lines at time $t_2 > t_1$.

For a constant population size ($x = 1$), the coalescent is invariant under time translations, $f_{nm}(t_1, t_2) = g_{nm}(t_2 - t_1)H(t_2 - t_1)$. Here $H(t) = 1$ if $t > 0$ and zero otherwise. The conditional probability $g_{nm}(t)$ was derived by TAVARÉ (1984). For $m \geq 2$ the result is:

$$g_{nm}(t) = \sum_{j=m}^n c_{nmj} e^{-bjt} \quad (18)$$

$$c_{nmj} = (-1)^{j-m} \frac{2j-1}{m!(j-m)!} \frac{\Gamma(m+j-1)}{\Gamma(m)} \frac{\Gamma(n)}{\Gamma(n+j)} \frac{\Gamma(n+1)}{\Gamma(n-j+1)}. \quad (19)$$

In the general case of a variable population size, as shown by GRIFFITHS and TAVARÉ (1994), the conditional probability depends only on the intensity $\Lambda(t_2) - \Lambda(t_1)$ during the time-interval $[t_1, t_2]$:

$$f_{nm}(t_1, t_2) = g_{nm}(\Lambda(t_2) - \Lambda(t_1)). \quad (20)$$

Now consider the case $k = 2$. For $i > j$ we have simply

$$\begin{aligned} \tau_i \tau_j &= \int_0^\infty dt_1 \mathbf{1}_{\{\ell(t_1)=i\}} \int_0^\infty dt_2 \mathbf{1}_{\{\ell(t_2)=j\}} \\ &= \int_0^\infty dt_1 \mathbf{1}_{\{\ell(t_1)=i\}} \int_{t_1}^\infty dt_2 \mathbf{1}_{\{\ell(t_2)=j\}}, \end{aligned} \quad (21)$$

because the second indicator function vanishes when $t_2 < t_1$. Averaging over realisations we find:

$$\langle \tau_i \tau_j \rangle = \int_0^\infty dt_1 f_{ni}(0, t_1) \int_{t_1}^\infty dt_2 f_{ij}(t_1, t_2). \quad (22)$$

This result is illustrated in Fig. 3b. In deriving it we have used the multiplicative rule

$$\langle \mathbf{1}_{\{\ell(t_1)=i\}} \mathbf{1}_{\{\ell(t_2)=j\}} \rangle = f_{ni}(0, t_1) f_{ij}(t_1, t_2). \quad (23)$$

For $i = j$, by contrast, we find

$$\begin{aligned}\tau_j^2 &= \int_0^\infty dt_1 \mathbf{1}_{\{\ell(t_1)=j\}} \int_0^\infty dt_2 \mathbf{1}_{\{\ell(t_2)=j\}} \\ &= 2 \int_0^\infty dt_1 \mathbf{1}_{\{\ell(t_1)=j\}} \int_{t_1}^\infty dt_2 \mathbf{1}_{\{\ell(t_2)=j\}},\end{aligned}\quad (24)$$

which upon averaging yields

$$\langle \tau_j^2 \rangle = 2 \int_0^\infty dt_1 f_{nj}(0, t_1) \int_{t_1}^\infty dt_2 f_{jj}(t_1, t_2). \quad (25)$$

More general correlation functions are readily obtained in terms of multiple integrals over the functions f_{nm} . Inserting into (15) we see that the combinatorial factors $(v_2!)^{-1} \dots (v_n!)^{-1}$ cancel to obtain

$$\langle T_n^k \rangle = k! \sum_{m_1=2}^n \sum_{m_2=2}^{m_1} \dots \sum_{m_k=2}^{m_{k-1}} m_1 \dots m_k \int_0^\infty dt_1 f_{nm_1}(0, t_1) \dots \int_{t_{k-1}}^\infty dt_k f_{m_{k-1}m_k}(t_{k-1}, t_k). \quad (26)$$

Eq. (26) provides an explicit expression for the moments of the total branch lengths T_n in populations with smooth population-size variations.

Note that Eq. (26) expresses the k -th moment of T_n in terms of a $2k$ -fold sum (according to (18) each factor of $f_{n_i m_i}$ contains a sum over j_i). Eq. (26) can be further simplified by explicitly performing the sums over m_1, \dots, m_k . This results in

$$\begin{aligned}\langle T_n^k \rangle &= k! \sum_{j_1=2}^n \dots \sum_{j_k=2}^{j_{k-1}} d_{n;j_1, \dots, j_k} \int_0^\infty dt_1 e^{-b_{j_1} \Lambda(t_1)} \int_{t_1}^\infty dt_2 e^{-b_{j_2} [\Lambda(t_2) - \Lambda(t_1)]} \\ &\quad \dots \int_{t_{k-1}}^\infty dt_k e^{-b_{j_k} [\Lambda(t_k) - \Lambda(t_{k-1})]}.\end{aligned}\quad (27)$$

The coefficients are determined by recursion:

$$d_{n;j} = \sum_{m=2}^j m c_{nmj} = (2j-1)(1+(-1)^j) \frac{\binom{2n-1}{n-j}}{\binom{2n-1}{n}}, \quad (28)$$

$$d_{n;j_1, \dots, j_k} = \sum_{m=j_2}^{j_1} m c_{nmj_1} d_{m;j_2, \dots, j_k}. \quad (29)$$

For the first moment, an expression corresponding to Eq. (26) for the particular case $k = 1$ was derived by SLATKIN (1996). Evaluating (26) for $k = 1$ using (27) and (28) we find

$$\langle T_n \rangle = \frac{1}{\binom{2n-1}{n}} \sum_{i=1}^{\lfloor n/2 \rfloor} (4i-1) \binom{2n-1}{n-2i} \int_0^\infty dt e^{-i(2i-1)\Lambda(t)}. \quad (30)$$

Here $\lfloor \dots \rfloor$ denotes taking the integer part. This result is equivalent to Eq. (3) in (AUSTERLITZ *et al.*, 1997), and also to the result obtained by summing Eq. (1) in (ZIVKOVIC and WIEHE, 2008). For $k = 2$, the coefficients $d_{n;j_1, j_2}$ are tabulated in Tab. I in appendix B for small values of n . In general, the nested integrals in Eq. (27) cannot be simplified further; their form expresses the correlations of the times τ_j due to population-size variations.

Finally note that for $n = 2$, Eq. (26) can be evaluated to give (14). We show this explicitly because it demonstrates how the expression (26) simplifies when $k > n$. We have

$$\begin{aligned}\langle \tau_2^k \rangle &= k! \int_0^\infty dt_1 f_{22}(0, t_1) \int_{t_1}^\infty dt_2 f_{22}(t_1, t_2) \dots \int_{t_{k-1}}^\infty dt_k f_{22}(t_{k-1}, t_k) \\ &= k! \int_0^\infty dt_1 \int_{t_1}^\infty dt_2 \dots \int_{t_{k-1}}^\infty dt_k f_{22}(0, t_k) = k \int_0^\infty dt t^{k-1} e^{-\Lambda(t)}.\end{aligned}\quad (31)$$

This yields Eq. (14).

We conclude this section by remarking that appendix A summarises an alternative approach to calculating $F_n(q)$ and the moments $\langle T_n^k \rangle$, again resulting in Eqs. (12) and (26). The approach described in appendix A yields a simple recursion, Eq. (A17),

which allows for a convenient calculation of the moments $\langle T_n^k \rangle$. This result also demonstrates explicitly how the moments $\langle T_n^k \rangle$, for a given curve $x(t)$, depend upon the time at which the population is sampled.

In the following two sections we describe a simple population model subject to population-size variations, and compare results of numerical simulations of this model to the analytical results obtained above.

IV. A MODEL FOR A POPULATION WITH TIME-DEPENDENT CARRYING CAPACITY

The purpose of this section is to describe a modified Wright-Fisher model with fluctuating population size. This model is used in the numerical simulations of sample genealogies described in Sec. V. Recall the three key assumptions of the Wright-Fisher model: (a) constant population-size, (b) discrete, non-overlapping generations, (c) a symmetric multinomial distribution of family sizes. We have adopted the following approach: in our simulations, assumptions (b) and (c) are still satisfied, but assumption (a) is relaxed.

We study a large but finite population of fluctuating size N_τ , where $\tau = 1, 2, \dots$ labels the discrete, non-overlapping generations forward in time. The model we have adopted is the following: consider a generation τ consisting of N_τ individuals. The number of individuals in generation $\tau + 1$ is then given by

$$N_{\tau+1} = \sum_{j=1}^{N_\tau} \xi_j \quad (32)$$

where the random family sizes ξ_j are independent and identically distributed random variables having a Poisson distribution with parameter λ_τ (specified below). Consequently the number $N_{\tau+1}$ is Poisson distributed with mean $N_\tau \lambda_\tau$.

This model exhibits a fluctuating population size N_τ , rapidly changing from generation to generation. As pointed out in the introduction, in large populations such fluctuations are averaged over by the ancestral coalescent process, and can be captured in terms of an effective population size. The resulting genealogies are simply described by Kingman's coalescent for a constant effective population size of the form (1).

Interesting population-size fluctuations occur on larger time scales, corresponding to 'slow' variations of the population size over several generations. Such slow changes are most commonly interpreted as consequences of a changing environment. A natural model for such changes is to impose a finite carrying capacity K_τ on the population which varies as a function of τ . This is the approach adopted in the following, and we choose

$$\lambda_\tau = \frac{1+r}{1+rN_\tau/K_{\tau+1}} \quad (33)$$

for a certain parameter value $r > 0$. Here $K_{\tau+1}$ is the carrying capacity in generation $\tau + 1$. If the environmental changes affected the population through fertility variations, $K_{\tau+1}$ would be replaced by K_τ in Eq. (33). Eq. (33) is chosen so that the population ceases to grow on average when the carrying capacity is reached ($\lambda_\tau = 1$ for $N_\tau = K_{\tau+1}$). When the population size is small, the population growth follows the logistic law, $\lambda_\tau = 1 + r(1 - N_\tau/K_{\tau+1})$, where r is the logistic growth rate. The particular form of Eq. (33) ensures that $\lambda_\tau > 0$.

Note that fluctuations of N_τ in this model are due to two different sources: rapid fluctuations are caused by the randomness of the family sizes, slow fluctuations are caused by the time dependence of the carrying capacity. Our choice for the time dependence of K_τ is dictated by the following considerations. The aim is to describe the influence of a fluctuating population size upon the statistics of genetic variation. To this end we need to consider the functional form of K_τ . A simple choice for K_τ is a periodically varying function, such as

$$K_\tau = K_0[1 + \varepsilon \sin(2\pi\nu\tau)]. \quad (34)$$

Note that a more complex dependence of K_τ upon τ can be obtained from superpositions of such functions with different amplitudes ε and frequencies ν . Here we use simply (34), and investigate how the statistics of genetic variation in a sample depends upon frequency of the fluctuations in K_τ .

Fig. 4 shows a realisation of a curve N_τ obtained in this manner (the choice of parameters is given in the figure caption). The figure clearly exhibits fluctuations in N_τ on two time scales. As pointed out above, we are interested in determining the effect of the size variations occurring at long time scales.

Last but not least we note that conditional on the sequence of population sizes, the genealogy of a set of individuals sampled at time τ can be determined recursively by randomly choosing ancestors in the preceding generations. This is ensured by the assumption that, conditioned on the values of N_τ and $N_{\tau+1}$, the family sizes follow a symmetric multinomial distribution $\text{Mn}(N_{\tau+1}; \frac{1}{N_\tau}, \dots, \frac{1}{N_\tau})$. The resulting correspondence with the Wright-Fisher rule of reproduction ensures that the genealogies can be determined recursively in the way suggested above.

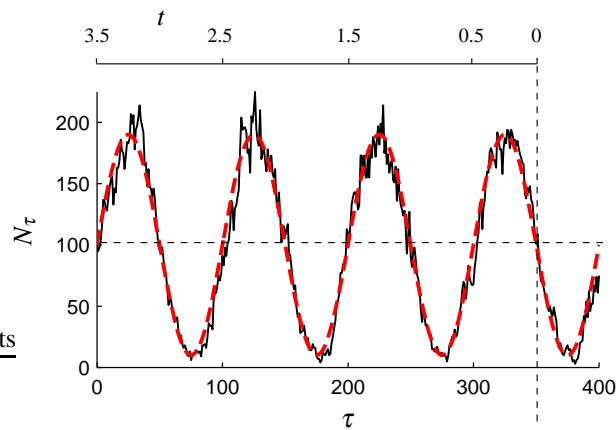


FIG. 4 Shows one realisation of the curve N_τ obtained from simulations of the model described in Sec. IV (black solid line). Choice of parameters: $r = 1$, $K_0 = 100$, $\varepsilon = 0.9$, and $K_0\nu = 1$. Also shown is an average over the fast fluctuations, $K_0[1 + \varepsilon \sin(2\pi\nu\tau)]$, red dashed line. The upper horizontal axis illustrates where the population is sampled, and how time is counted backwards in the coalescent approximation. N_0 denotes the size of the population at the time of sampling.

V. COMPARISON BETWEEN NUMERICAL SIMULATIONS AND COALESCENT PREDICTIONS

In this section we discuss the numerically computed distributions shown in Fig. 1 in terms of the results obtained using the coalescent approximation. The shapes observed in Fig. 1 are conveniently characterised in terms their mean $\langle T_n \rangle$, variance, skewness, and kurtosis:

$$\text{var}(T_n) = \langle T_n^2 \rangle - \langle T_n \rangle^2,$$

$$\text{skew}(T_n) = \frac{\langle (T_n - \langle T_n \rangle)^3 \rangle}{\text{var}^{3/2}(T_n)}, \quad (35)$$

$$\text{kurt}(T_n) = \frac{\langle (T_n - \langle T_n \rangle)^4 \rangle}{\text{var}^2(T_n)}. \quad (36)$$

Recall that for a normal distribution the skewness vanishes, and the kurtosis equals three. We can write the skewness and kurtosis in terms of the moments $\langle T_n^k \rangle$ using $\langle (T_n - \langle T_n \rangle)^3 \rangle = \langle T_n^3 \rangle - 3\langle T_n^2 \rangle \langle T_n \rangle + 2\langle T_n \rangle^3$ and $\langle (T_n - \langle T_n \rangle)^4 \rangle = \langle T_n^4 \rangle - 4\langle T_n^3 \rangle \langle T_n \rangle + 6\langle T_n^2 \rangle \langle T_n \rangle^2 - 3\langle T_n \rangle^4$.

As argued in Sec. IV and as shown in Fig. 4, our model populations exhibit fast size changes due to the random distribution of family sizes. As pointed out in the introduction, these fluctuations are averaged over by the genealogical process and need not be considered. The model populations are also subject to slow (and deterministic) size fluctuations given by the time-dependence (34) of the carrying capacity. Averaging over the fast fluctuations these give rise to a smooth population-size dependence $x(t)$. Given Eq. (34), the distribution of T_n depends upon the instance in time when the population is sampled. In the simulations we sampled at a particular point (illustrated in Fig. 4 as a dashed vertical line), so that

$$x(t) = 1 + \varepsilon \sin(\omega t). \quad (37)$$

Here the frequency is given by $\omega = 2\pi\nu K_0$, and time t is now counted backwards, as in Sec. III. If the population were sampled at a different time, the distribution $\rho(T_n)$ of T_n (and hence its moments and the corresponding function $F_n(q)$) would change: the distribution depends for example upon whether most recently the population was expanding or declining. The results derived in appendix A make it possible to determine the corresponding changes to $\rho(T_n)$ in a transparent manner, but we do not discuss this issue further here.

Fig. 5 shows how the mean, variance, skewness, and kurtosis of the distribution of T_n depend on the frequency ω of the population size variation, Eq. (37). Shown are results of numerical simulations of the model described in section IV (symbols), and results obtained within the coalescent approximation using Eq. (A17). We observe that the coalescent approximation describes the results of the numerical simulations well, even for small population sizes.

In the numerical simulations we have found that, for very small population sizes, random fluctuations of N_τ around the time-dependent carrying capacity K_τ become increasingly important. Since we suspected that the small deviations observed in Fig. 5a for $K_0 = 100$ were due to such fluctuations, we performed slightly modified simulations imposing a deterministic law upon N_τ by forcing $N_\tau = K_\tau$ in every generation (where K_τ is given by (34)). Comparison of the corresponding results (not shown) with Fig. 5a indicates that the deviations for $K_0 = 100$ at large frequencies are indeed caused by the stochastic fluctuations in

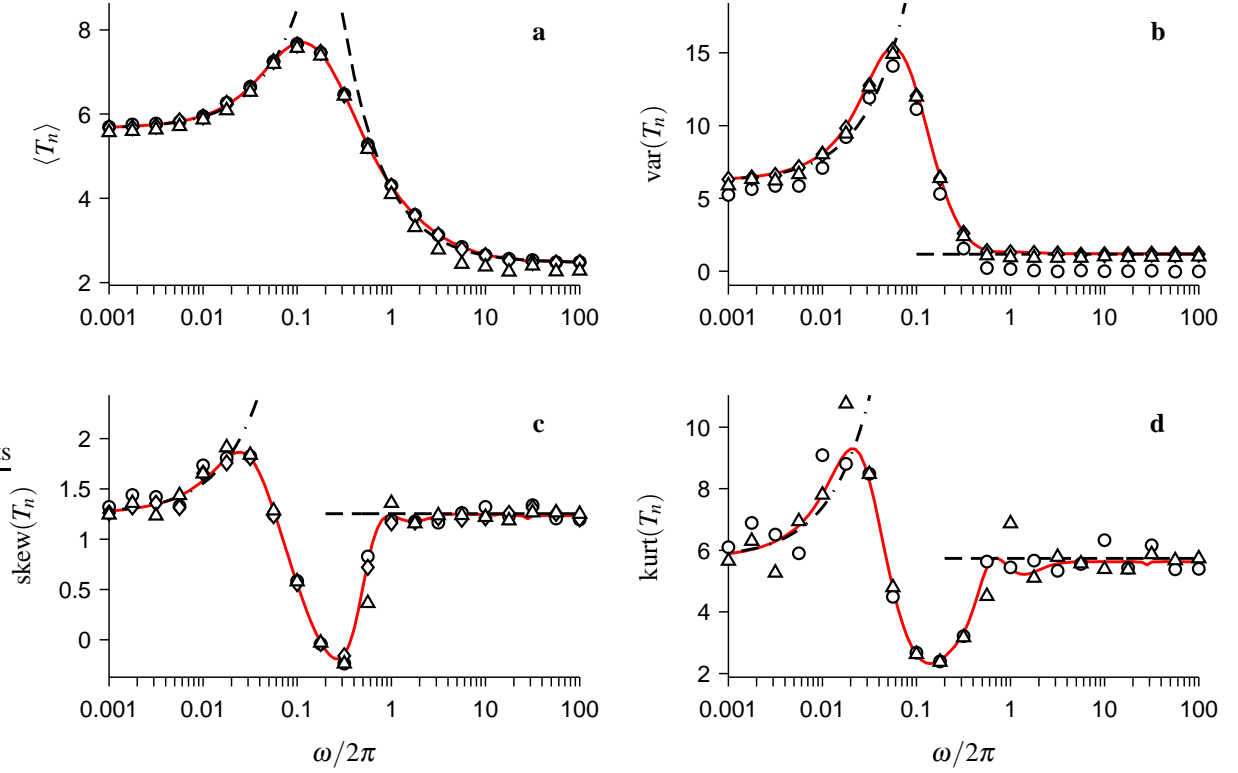


FIG. 5 Shows mean (a), variance (b), skewness (c) and kurtosis (d) of the distribution of T_n for samples of size $n = 10$, as a function of the frequency of the population-size fluctuations. Shown are results of numerical simulations (10,000 simulations, $K_0 = 100$, triangles; $K_0 = 1,000$, diamonds; and $K_0 = 10,000$, circles) as well as results computed within the coalescent approximation described in Sec. III, red solid lines. Black dash-dotted and dashed lines show the approximations for small frequencies, Eqs. (40) and (42), and for large frequencies, Eqs. (47) and (48). The expressions for the limiting behaviours of the skewness and the kurtosis are shown in panels c and d, but are not given in the text. The remaining parameter values are $r = 1$ and $\varepsilon = 0.9$, as in Fig. 1.

the population dynamics underlying Fig. 5a. A different interpretation of this effect is the following: when the population size is very small, and when ε is close to unity, the population may exhibit a non-negligible probability of becoming extinct during the expected time to the most recent common ancestor for a sample of size n . In this case we have conditioned on the existence of the population during $100K_0$ generations using rejection sampling. In practice this avoids extinction, but it leads to a biased size distribution.

Consider now the frequency dependence of the moments shown in Fig. 5. It can be qualitatively and quantitatively understood using Eq. (27) together with the following expression for $\Lambda(t)$:

$$\Lambda(t) = \int_0^t \frac{ds}{1 + \varepsilon \sin(\omega s)} = \frac{\left\lfloor \frac{\omega t}{2\pi} + \frac{1}{2} \right\rfloor - \frac{1}{\pi} \arctan\left(\frac{\varepsilon}{\sqrt{1-\varepsilon^2}}\right) + \frac{1}{\pi} \arctan\left(\frac{\tan(\omega t/2) + \varepsilon}{\sqrt{1-\varepsilon^2}}\right)}{(\omega/2\pi)\sqrt{1-\varepsilon^2}}. \quad (38)$$

We discuss the limits of small and large frequencies ω separately. In the limit of $\omega \rightarrow 0$, Eq. (38) simplifies to $\Lambda(t) \approx t - \frac{1}{2}\varepsilon\omega t^2$. Inserting this into (30) and approximating

$$\int_0^\infty dt e^{-b_j \Lambda(t)} \approx \frac{1}{b_j} \left(1 + \frac{\varepsilon\omega}{b_j}\right) \quad (39)$$

we find

$$\langle T_n \rangle \approx 2h_n + 4\varepsilon\omega(g_n - h_n/n). \quad (40)$$

Here $h_n = \sum_{j=1}^{n-1} j^{-1}$ and $g_n = \sum_{j=1}^{n-1} j^{-2}$. Eq. (40) is shown in Fig. 5a as a dash-dotted line. To compute the variance we

approximate

$$\int_0^\infty dt_1 e^{-b_{j_1} \Lambda(t_1)} \int_{t_1}^\infty dt_2 e^{-b_{j_2} [\Lambda(t_2) - \Lambda(t_1)]} \approx \frac{1}{b_{j_1} b_{j_2}} + \varepsilon \omega \frac{b_{j_1} + 2b_{j_2}}{b_{j_1}^2 b_{j_2}^2}, \quad (41)$$

and find an approximate expression for $\langle T_n^2 \rangle$ which results in the following expression for the variance:

$$\text{var}(T_n) \approx 4g_n + 16\varepsilon\omega \left(f_n - g_n + \frac{h_n - g_n}{n} \right) \quad (42)$$

with $f_n = \sum_{m=1}^{n-1} (m^{-3} + m^{-2} h_{m+1})$. The limiting value for zero frequency is that of the standard coalescent with constant population size $x = 1$. Eq. (42) is shown in Fig. 5b as a dash-dotted line. Similarly the standard results for the constant-size coalescent are obtained for the skewness and for the kurtosis in the limit of $\omega \rightarrow 0$. This limiting behaviour is illustrated in Fig. 1a which shows that the distribution of T_n approaches that for Kingman's coalescent for a constant population size $x = 1$ in the limit of small frequencies. We note that for $\omega \ll 1$, the population-size dependence is essentially that of a declining population, because the time to the most recent common ancestor is reached before the first maximum in $x(t)$ going backwards in time (see Fig. 4 and Eq. (37)).

Of particular interest is the limit of large frequencies, as we now show. As the frequency tends to infinity, one expects that the coalescent process averages over the population-size oscillations, and the standard coalescent process with a constant effective population size should be obtained. For large but finite frequencies, by contrast, Fig. 5a exhibits deviations from the standard coalescent behaviour. In the following we analyse the behaviour of the moments in this regime. In the limit of large frequencies, Eq. (38) simplifies to

$$\Lambda(t) = \frac{t}{\sqrt{1-\varepsilon^2}} - \frac{\arctan\left(\frac{\varepsilon}{\sqrt{1-\varepsilon^2}}\right)}{\omega\sqrt{1-\varepsilon^2}} + O(\omega^{-2}) + \text{oscillatory terms}. \quad (43)$$

For large frequencies, the function $\Lambda(t)$ is well approximated by a shifted linear function

$$\Lambda(t) \approx t/x_{\text{eff}} + \bar{\Lambda}_0. \quad (44)$$

Here

$$x_{\text{eff}} = \left(\lim_{T \rightarrow \infty} \frac{1}{T} \int_0^T \frac{dt}{1 + \varepsilon \sin(\omega t)} \right)^{-1} = \sqrt{1 - \varepsilon^2} \quad (45)$$

is the effective population size according to Eq. (1), it describes the influence of the demographic fluctuations upon the part of the genealogy in the far past. The small offset

$$\bar{\Lambda}_0 = -\frac{\arctan(\varepsilon/\sqrt{1-\varepsilon^2})}{x_{\text{eff}}\omega} \approx -\frac{\varepsilon}{x_{\text{eff}}\omega} \quad \text{for } \varepsilon \text{ not too close to unity} \quad (46)$$

describes the influence of demographic changes on the most recent part of the genealogy. Inserting the approximation (44) into (27) we find for large frequencies (and when the amplitude ε is not too close to unity):

$$\langle T_n \rangle \approx 2x_{\text{eff}}h_n + \frac{n\varepsilon}{\omega}. \quad (47)$$

The first term in (47) is the expected time of Kingman's coalescent for a constant effective population size x_{eff} . The curve corresponding to (47) is shown as a dashed line in Fig. 5a.

We now discuss the behaviour of the variance shown in Fig. 5b. For the second moment we find:

$$\langle T_n^2 \rangle \approx 4x_{\text{eff}}^2(g_n + h_n^2) + \frac{4nh_n x_{\text{eff}} \varepsilon}{\omega}, \quad (48)$$

The first term in Eq. (48) corresponds to the second moment of T_n in Kingman's coalescent with a constant effective population size x_{eff} . The second term in (48) represents a correction due to finite but large frequencies, it depends in a simple fashion on the effective population size x_{eff} and on the sample size n .

Comparing Eqs. (47) and (48) we arrive at the conclusion that the corresponding correction for the variance $\text{var}(T_n)$ vanishes. This is consistent with the fact that, at large frequencies, the variance of T_n is surprisingly insensitive to changes in frequency

(as opposed to the behaviour of $\langle T_n \rangle$, see Fig. 5a and b). In fact, the limiting value (shown in Fig. 5b as a dashed line) is a very good approximation to $\text{var}(T_n)$ down to $\omega \approx 3$.

Consider now the skewness and the kurtosis shown in Figs. 5c and d. Their behaviour is similar to that of the variance: over a substantial range, the skewness and the kurtosis are essentially independent of ω . The results shown in Fig. 5 imply that over a large range of frequencies, the distribution of the total branch lengths T_n can be approximated as follows: the distribution is essentially that of the standard Kingman coalescent with an effective population size x_{eff} , but the distribution is shifted such that its mean is given by Eq. (47), rather than by $2x_{\text{eff}}h_n$.

One may wonder when this ‘rigid shift’ occurs. Given Eq. (26) it is straightforward to work out the fluctuations of the times τ_j within the approximation (44). We find that for $j < n$, the expected value of τ_j is exactly that of the standard Kingman coalescent with effective population size x_{eff} . But for $j = n$ it is rigidly shifted by $-x_{\text{eff}}\bar{\Lambda}_0$. This indicates that the genealogies are essentially those of the standard coalescent, but modified by an initial rigid shift. In the parameter regime discussed here, the distribution of times is expected to be well approximated by a two-parameter family of distributions:

$$P(T_n < z) \approx \left[1 - \exp\left(-\frac{z/x_{\text{eff}} + n\bar{\Lambda}_0}{2}\right) \right]^{n-1} \quad (49)$$

when $z/x_{\text{eff}} > -n\bar{\Lambda}_0$, and $P(T_n < z) \approx 0$ for smaller values of z . The first parameter is the effective population size x_{eff} which determines the slope of the function $\Lambda(t)$ at large times and describes the demographic effect on the far past of the genealogy. The second parameter, $\bar{\Lambda}_0$ describes the influence of the demographic fluctuations on the initial part of the sample genealogy. This parameter can be negative (initial population expansion, this is the case shown in Fig. 5) or positive (initial population decline). When $\bar{\Lambda}_0 > 0$, the distribution $\rho(T_n)$ is rigidly shifted to the left. In this case the approximation (44) is expected to break down when the body of the distribution reaches $T_n = 0$.

Note that the distribution (49) cannot be described by a single parameter (a ‘generalised effective population size’). The approximation (49) was used to generate the red dashed curves in Fig. 1d and e.

VI. DISCUSSION AND CONCLUSIONS

The aim of this paper was to investigate how the frequency of smooth population-size fluctuations determines the shape of the distribution of total branch lengths of sample genealogies, and thus of statistical measures of genetic variation.

We have performed simulations for a modified Wright-Fisher model of a population subject to a time-periodically varying carrying capacity and have determined the distribution of the total branch lengths, shown in Fig. 1. We have characterised how the shapes of the distributions depend upon the frequency of the population size fluctuations by computing the frequency dependence of the moments of these distributions. We could explain these dependencies in terms of coalescent approximations. In particular, we derived a general expression – Eq. (27) – for the moments $\langle T_n^k \rangle$ in populations subject to smooth population changes of otherwise arbitrary form.

Our results show how quickly (or slowly) the standard coalescent result for a constant (effective) population sizes is recovered in the limits of large and small frequencies. More importantly, our coalescent results allow to determine how significant deviations are at large but finite frequencies. In this case we have argued that at large frequencies, the distribution of T_n is essentially that of the standard Kingman coalescent with an effective population size x_{eff} , but with a shifted mean value

$$\langle T_n \rangle = 2x_{\text{eff}} \sum_{j=1}^{n-1} \frac{1}{j} + \frac{n\varepsilon}{\omega}. \quad (50)$$

The first term on the rhs corresponds to the result of the standard Kingman coalescent with constant effective population size x_{eff} . The second term on the rhs is the correction term resulting from the population-size variations (ε is the amplitude of the population-size oscillations, ω its frequency, and n is the sample size). Last but not least we have found that the coalescent approximation yields a reliable description of the numerical data, even for very small populations.

These results enable us to determine how the distribution of the number S_n of mutations (single-nucleotide polymorphisms) in a sample of size n depends upon the frequency and on the amplitude of population-size fluctuations: Eq. (4) allows to compute moments of S_n from Eq. (27). In this way we have determined the mean, variance, skewness, and the kurtosis of the distribution of S_n . The results are shown in Figs. 6 and 7. As expected, the moments of S_n approach those of $\theta T_n/2$ as the scaled mutation parameter θ increases. This can be verified by comparing the red curves (corresponding to $\varepsilon = 0.9$) in Fig. 7 to the red curves in Fig. 5. The higher moments converge more slowly than the mean and the variance. In conclusion, Figs. 6 and 7 demonstrate that the distribution of the number S_n of mutations in samples of size n depends in a complex manner on the amplitude and on the frequency of the population-size variations, and on the mutation parameter θ .

We close with a number of remarks. First, Eq. (27) is easily generalised to describe the moments of observables which are polynomial functions of the times τ_j (see Fig. 3a for a definition of these times). Particularly simple is the case of observables

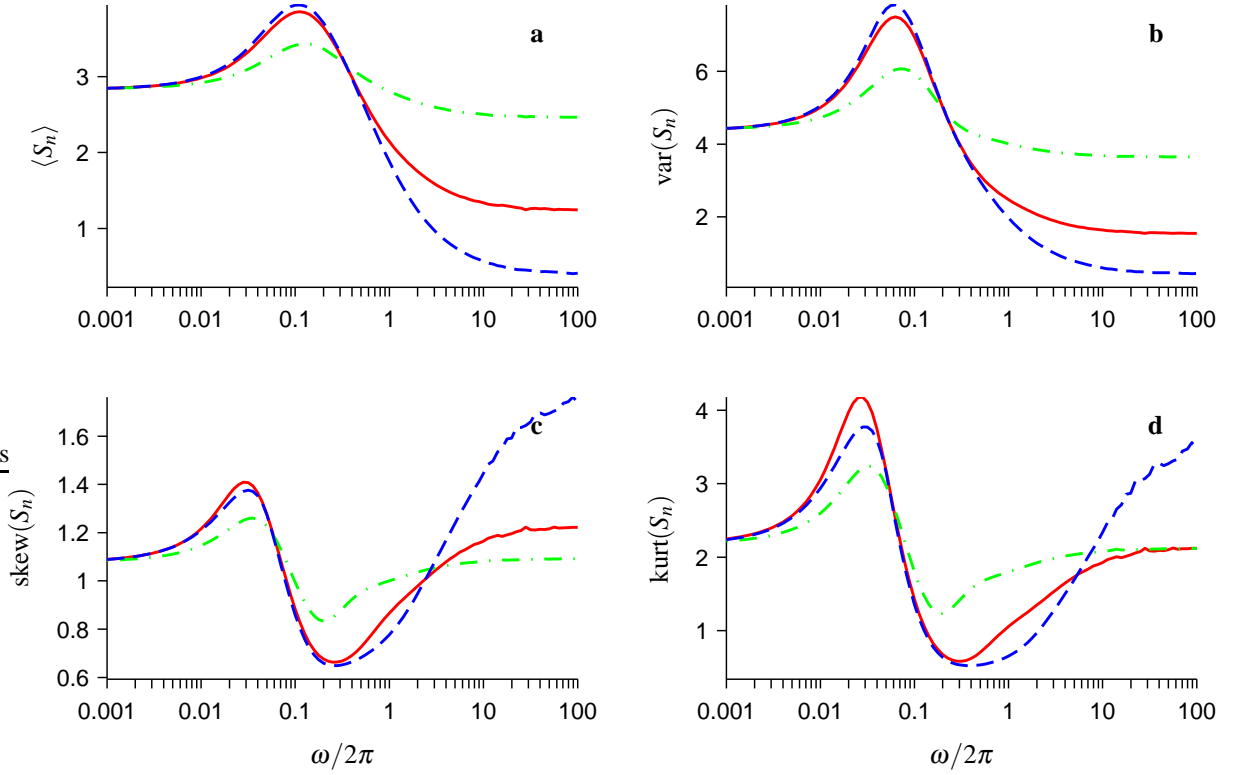


FIG. 6 Shows mean (a), variance (b), skewness (c) and kurtosis (d) of the distribution of S_n for samples of size $n = 10$ and scaled mutation parameter $\theta = 1$, as a function of the frequency of the population-size fluctuations, for three values of ϵ : $\epsilon = 0.5$ (dashed-dotted green lines), $\epsilon = 0.9$ (solid red lines), and $\epsilon = 0.99$ (dashed blue lines). The curves were obtained by iteration of Eq. (A17) in combination with (38).

A that are linear functions of the times τ_j , $A_n = \sum_{j=2}^n a_j \tau_j$. In this case the k -th moment of A_n is given by Eq. (27), but with modified coefficients: the factors m in Eqs. (28) and (29) are replaced by a_m .

Second, some observables (such as the F-statistic (FU and LI, 1993)) can be written as linear functions of τ_j , but with random coefficients. In this case too it is possible to explicitly compute the moments of the distribution of the observable. These two questions are addressed in a separate paper (SAGITOV *et al.*, 2010).

Third, a result derived in appendix A, Eq. (A17), allows us to determine in a transparent fashion how the fluctuations of T_n and other observables depend upon the time at which the population is sampled. This will make it possible to discuss for example how Tajima's D -statistic or the F -statistic depend upon the time of sampling after a bottleneck, a population expansion, or a decline.

Fourth, population-size fluctuations are sampled non-uniformly by the genealogies: initial coalescent events occur at faster rates and are thus more sensitive to recent size fluctuations. Remote coalescent events, by contrast, occur at slower rates thus damping the effect of size fluctuations in the far past. We therefore expect significant deviations from the standard coalescent behaviour arising from the most recent history for large sample sizes n . It would be interesting to quantify this expectation by computing the covariances and higher moments of the times τ_j during which the sample genealogy has j lines: first for large $i \approx n$ and $j \approx n$ we expect to observe strong correlations $\langle \tau_i \tau_j \rangle - \langle \tau_i \rangle \langle \tau_j \rangle$ and thus deviations from the coalescent. Second for small values of i and j we expect the times τ_i and τ_j to de-correlate and to follow the distribution of the standard coalescent (with an effective population size).

Fifth, the model introduced in Sec. IV assumes a carrying capacity that varies sinusoidally, with a single frequency. It turns out, however, that our findings are valid for arbitrary time-dependent fluctuations with sufficiently strong modes at small frequencies. Examples are linear combinations of high-frequency oscillations, or stochastic fluctuations around a constant population size with sufficiently short auto-correlation time. In this more general case, too, we expect that $\Lambda(t)$ is well approximated by (44). If this is the case, the distribution of times is of the form (49) when $\bar{\Lambda}_0$ is small.

Taken together, the results derived in this paper give a rather complete understanding of the fluctuations of empirical observables due to smooth population size variations. These results will be significant when attempting to disentangle the effects of population-size variations from other factors influencing genetic variation.

Our results raise the question under which circumstances the deviations from standard coalescent behaviours due to population-size fluctuations (Figs. 1, 5, 6, and 7) are most likely to strongly affect the interpretation of empirical data. As our analysis indicates, the deviations become substantial when the frequency $\omega = 2\pi\nu K_0$ is of the order of or less than the

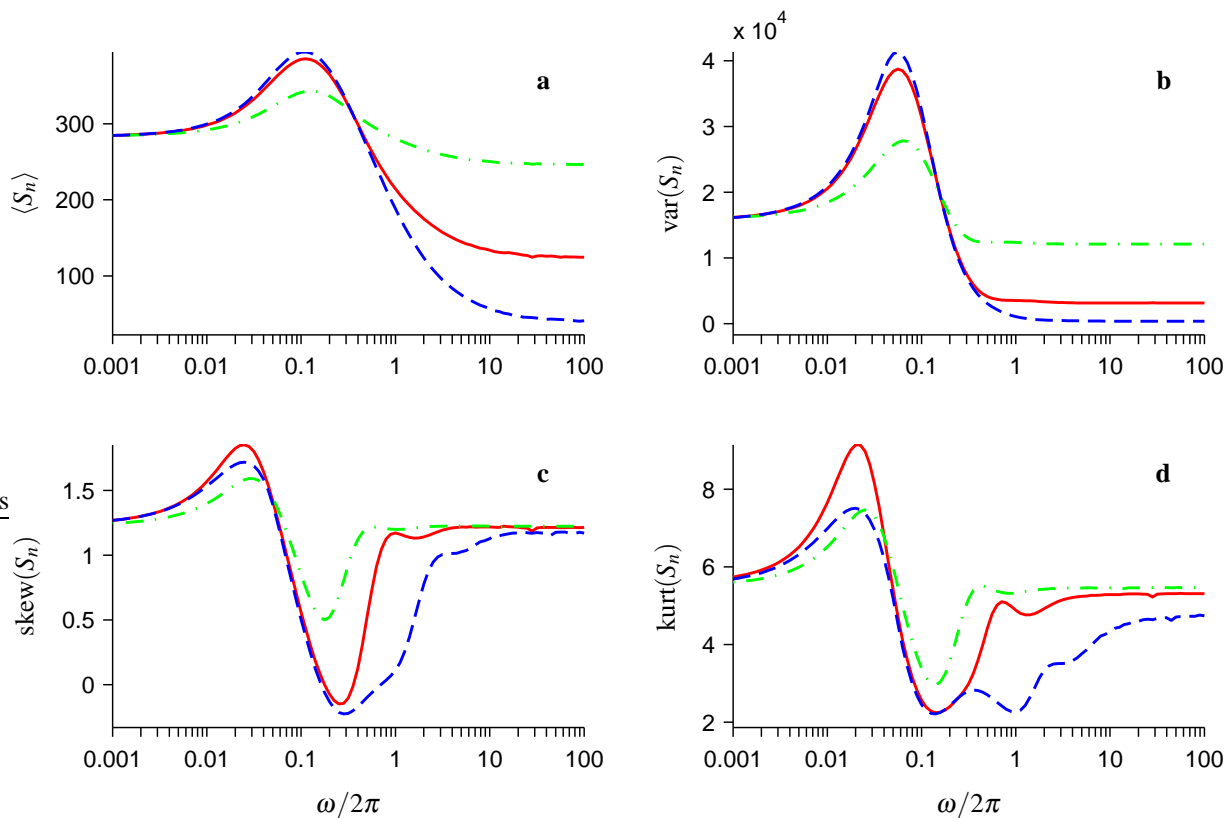


FIG. 7 Same as Fig. 6, but for $\theta = 100$.

inverse expected time between coalescent events in the sample. Here ν is the frequency of the population size variations, Eq. (37), and K_0 is a suitable measure of the population size (the arithmetically averaged carrying capacity in our example). In other words, rapid population-size fluctuations will have the strongest effect (other than simply determining the effective population size, Eq. (1)) in small local sub-populations with restricted gene flow between sub-populations with different fluctuations. The deviations are expected to be smaller at larger spatial scales, because the ancestral process averages over the spatial fluctuations. More generally, we conclude that deviations from standard coalescent behaviour are expected for populations subject to an environment which smoothly changes as a function of space and time. An example for such a population is the marine snail *L. saxatilis*. Its habitat on the Northern coast of Bohuslän (Sweden) is fragmented into sub-populations with strongly restricted gene flow between them, effective population sizes of sub populations have been found to be very small (JOHANNESSON, 2009). Starting from the results derived in this paper, we hope to determine gene genealogies in such fragmented populations subject to smooth variations of population size in space and time.

Acknowledgements. Support from Vetenskapsradet, The Bank of Sweden Tercentenary Foundation, and from the Centre for Theoretical Biology at the University of Gothenburg are gratefully acknowledged.

References

- AUSTERLITZ, B., B. JUNG-MULLER, B. GODELLE, and P. GOUYON, 1997 Evolution of coalescence times, genetic diversity and structure during colonization. *Theor. Pop. Biol.* **51**: 148–164.
- EWENS, W., 1982 The concept of the effective population size. *Theor. Popul. Biol.* **21**: 373–378.
- FISHER, R. A., 1930 *The genetical theory of natural selection*. Clarendon, Oxford.
- FU, Y., and W. LI, 1993 Statistical tests of neutrality of mutations. *Genetics* **133**: 693–709.
- GARRIGAN, D., and M. F. HAMMER, 2006 Reconstructing human origins in the genomic era. *Nat. Rev. Genet.* **7**: 669–680.
- GRIFFITHS, R., and S. TAVARÉ, 1994 Sampling theory for neutral alleles in a varying environment. *Phil. Trans. Roy. Soc. Lon. B* **344**: 403–410.
- JAGERS, P., and S. SAGITOV, 2004 Convergence to the coalescent in populations of substantially varying size. *Journal of Applied Probability* **41**: 368–378.
- JOHANNESSON, K., 2009 private communication .
- KAJ, I., and S. KRONE, 2003 The coalescent process in a population with stochastically varying size. *J. Appl. Prob.* **40**: 33–48.

- KIMMEL, M., and R. CHAKRABORTY, 1996 Measures of variation at DNA repeat loci under a general stepwise mutation model. *Theoretical Population Biology* **50**: 345–367.
- KINGMAN, J., 1982 The coalescent. *Stoch. Proc. Appl.* **13**: 235–248.
- MORAN, P., 1958 Random processes in genetics. *Proc. Cambridge Philos. Soc.* **54**: 60–71.
- NORDBORG, M., and S. KRONE, 2003 *Modern Developments in Population Genetics: The Legacy of Gustave Malécot*. Oxford University Press, Oxford, 194–232.
- OHTA, T., and M. KIMURA, 1973 A model of mutation appropriate to estimate the number of electrophoretically detectable alleles in a finite population. *Genet Res* **22**: 201–204.
- SAGITOV, S., M. RAFAJLOVIC, B. MEHLIG, and A. ERIKSSON, 2010 External branch lengths of genealogies in expanding and in declining populations. unpublished .
- SJÖDIN, P., I. KAJ, S. KRONE, M. LASCOUX, and M. NORDBORG, 2005 On the meaning and existence of an effective population size. *Genetics* **169**: 1061–1070.
- SLATKIN, M., 1996 Gene genealogies within mutant allelic classes. *Genetics* **143**: 579–587.
- TAJIMA, F., 1989 Statistical method for testing the neutral mutation hypothesis by DNA polymorphism. *Genetics* **123**: 585–595.
- TAVARÉ, S., 1984 Evolution of coalescence times, genetic diversity and structure during colonization. *Theor. Pop. Biol.* **26**: 119–164.
- TAVARÉ, S., 2004 *Ancestral Inference in Population Genetics*. Springer, Berlin, 1–188.
- WAKELEY, J., and O. SARGSYAN, 2009 Extensions of the coalescent effective population size. *Genetics* **181**: 341–345.
- WATTERSON, G. A., 1975 On the number of segregation sites in genetical models without recombination. *Theor. Pop. Biol.* **7**: 256–276.
- WRIGHT, S., 1931 Evolution in mendelian populations. *Genetics* **16**: 97–159.
- ZENG, K., Y. FU, S. SHI, and C. WU, 2006 Statistical tests for detecting positive selection by utilizing high-frequency variants. *Genetics* **174**: 1431–1439.
- ZIVKOVIC, D., and T. WIEHE, 2008 Second-order moments of segregating sites under variable population size. *Genetics* **180**: 341–357.

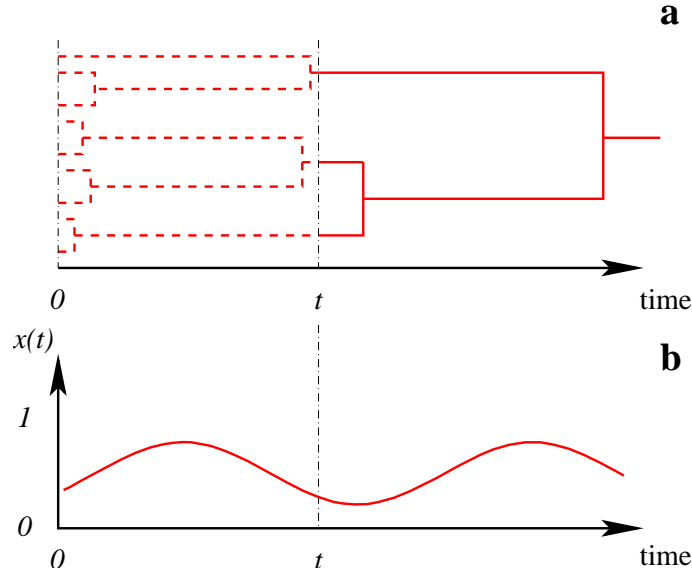


FIG. 8 **a** Illustrates the definition of $F_n(q, t)$ which for $q = \theta/2$ is the probability that n sequences sampled at time t are identical. The corresponding branches in the tree are drawn as solid lines, and $n = 3$ in the figure. **b** Shows schematically how the population size $x(t)$ depends upon time.

APPENDIX A: Alternative calculation of $F_n(q)$ and $\langle T_n^k \rangle$

In this appendix we demonstrate an alternative way of calculating function $F_n(q)$ and the moments $\langle T_n^k \rangle$ within the coalescent approximation. Given a realisation of the curve $x(t)$, the function $F_n(q)$ can be calculated as follows.

Consider the function $F_n(q, t)$ that is, for $q = \theta/2$, the probability that n sequences sampled at time t are identical. The time argument describes how F_n depends upon the time at which the population is sampled, given a smooth population-size curve $x(t)$. The definition of $F_n(q, t)$ is illustrated for the case $n = 9$ in Fig. 8. In Secs. III and V, the populations were sampled at $t = 0$, which corresponds to the choice $F_n(q) = F_n(q, 0)$. The more general quantity $F_n(q, t)$ allows to determine how the fluctuations of sample genealogies depend upon the time of sampling (in a population of constant size, F_n is independent of t).

To obtain a recursion for $F_n(q, t)$ in a population of fluctuating size, take $q = \theta/2$ and consider a small time interval δt . A change in F_n during this time interval is due to either a mutation in one of the ancestral lines, or to two ancestral lines having a common ancestor. Thus, to first order in δt

$$F_n(q, t) = \left[1 - nq\delta t - \frac{n(n-1)}{2x(t)}\delta t \right] F_n(q, t + \delta t) + \frac{n(n-1)}{2x(t)}\delta t F_{n-1}(q, t + \delta t). \quad (\text{A1})$$

Taking the limit $\delta t \rightarrow 0$, we obtain:

$$\frac{\partial}{\partial t} F_n(q, t) = \left[nq + \frac{n(n-1)}{2x(t)} \right] F_n(q, t) - \frac{n(n-1)}{2x(t)} F_{n-1}(q, t). \quad (\text{A2})$$

The recursion is terminated by $F_1(q, t) \equiv 1$ for all values of t . In a population of constant size $x = 1$, $F_n(q, t)$ does not depend upon t and the result (7) is immediately recovered from (A2). To find the general solution, Eq. (A2) is rewritten as follows:

$$F_n(q, t) = b_n \int_t^\infty \frac{ds}{x(s)} e^{nq(t-s) + b_n[\Lambda(t) - \Lambda(s)]} F_{n-1}(q, s). \quad (\text{A3})$$

It is convenient to consider the function $G_n(q, t) = e^{-nqt - b_n\Lambda(t)} F_n(q, t)$. It obeys the recursion

$$G_n(q, t) = b_n \int_t^\infty \frac{ds}{x(s)} e^{-qs - (n-1)\Lambda(s)} G_{n-1}(q, s) \equiv (\mathcal{L}_n \phi G_{n-1})(t). \quad (\text{A4})$$

Here \mathcal{L}_k is the operator

$$(\mathcal{L}_k f)(t) = b_k \int_t^\infty \frac{ds}{x(s)} e^{-(k-1)\Lambda(s)} f(s), \quad (\text{A5})$$

and $\phi(s) = \exp(-qs)$. In terms of this operator, the recursion is simply solved by repeated action of \mathcal{L}_k on the function ϕ :

$$G_n(q, t) = (\mathcal{L}_n \phi \mathcal{L}_{n-1} \cdots \phi \mathcal{L}_2 \phi^2)(t), \quad (\text{A6})$$

where we have used the fact that $G_1(q, s) = \exp(-qs)$. Noting that $G_n(q, 0) = F_n(q, 0) \equiv F_n(q)$ we obtain the desired expression (12) for $F_n(q)$:

$$F_n(q) = (\mathcal{L}_n \phi \mathcal{L}_{n-1} \cdots \phi \mathcal{L}_2 \phi^2)(0). \quad (\text{A7})$$

The moments $\langle T_n^k \rangle$ can be calculated in a similar fashion. Consider the function $\langle T_n^k(t) \rangle$ describing the moments of the total length of all solid branches shown in Fig. 8. Then $\langle T_n^k \rangle = \langle T_n^k(0) \rangle$, and $\langle T_n^k(t) \rangle$ obeys the recursion:

$$\frac{\partial}{\partial t} \langle T_n^k(t) \rangle = -kn \langle T_n^{k-1}(t) \rangle + \frac{b_n}{x(t)} [\langle T_n^k(t) \rangle - \langle T_{n-1}^k(t) \rangle]. \quad (\text{A8})$$

We introduce the function $h_n^{(k)}(t) = e^{-b_n \Lambda(t)} \langle T_n^k(t) \rangle$. With the initial conditions $h_n^{(0)}(t) = e^{-b_n \Lambda(t)}$ for $n \geq 2$ and $h_1^{(m)}(t) = 0$ for $m \geq 1$, the recursion (A8) is simply:

$$h_n^{(k)}(t) = k \sum_{m=2}^n m (\mathcal{L}_n \mathcal{L}_{n-1} \cdots \mathcal{L}_{m+1} \mathcal{I} h_m^{(k-1)})(t) \quad (\text{A9})$$

where \mathcal{I} is the integral operator $\int_t^\infty dt'$.

Now we show that the action of the chain $\mathcal{L}_n \mathcal{L}_{n-1} \cdots \mathcal{L}_{m+1}$ of operators on an arbitrary function f can be represented in terms of a single integral. To show this, it is convenient to make a change of variables to $z = \Lambda(t)$:

$$(\mathcal{L}_k f)(z) = b_k \int_z^\infty dy e^{-(k-1)y} f(y). \quad (\text{A10})$$

The task is to seek a kernel $K_{nm}(z, z')$ such that for any function f

$$(\mathcal{L}_n \mathcal{L}_{n-1} \cdots \mathcal{L}_m f)(z) = \int_z^\infty dz' K_{nm}(z, z') f(z'). \quad (\text{A11})$$

The kernel must satisfy

$$K_{nm}(z, z') = b_n \int_z^{z'} dy e^{-(n-1)y} K_{n-1, m}(y, z') \quad (\text{A12})$$

Together with the initial condition $K_{mm}(z, z') = b_m \exp[-(m-1)z'] H(z' - z)$, this recursion allows to compute the kernel in closed form. This can for example be achieved by considering the Laplace transform of (A10). We find:

$$K_{nm}(z, z') = \sum_{j=m}^n k_{nmj} e^{-(b_n - b_j)z} e^{(b_{m-1} - b_j)z'} \quad (\text{A13})$$

$$k_{nmj} = (-1)^{j-m} \frac{2j-1}{2} \frac{\Gamma(m+j-1)}{\Gamma(m)\Gamma(m-1)\Gamma(j-m+1)} \frac{\Gamma(n)\Gamma(n+1)}{\Gamma(n+j)\Gamma(n-j+1)}.$$

This kernel can be used to evaluate (A9). For any function $g(t)$ we have that

$$(\mathcal{L}_n \cdots \mathcal{L}_{m+1} \mathcal{I} g)(t) = \int_t^\infty dt' A_{nm+1}(\Lambda(t), \Lambda(t')) g(t') \quad (\text{A14})$$

with

$$A_{nm+1}(z, z') = \int_z^{z'} dz'' K_{nm+1}(z, z'') \quad (\text{A15})$$

(and $A_{nm+1}(z, z') = 1$). Inserting this result into (A9) yields

$$h_n^{(k)}(t) = k \sum_{m=2}^n m \int_t^\infty dt' A_{nm+1}(\Lambda(t'), \Lambda(t)) h_m^{(k-1)}(t'). \quad (\text{A16})$$

Identifying $A_{nm+1}(z, z') = \exp(-b_n z) g_{nm}(z' - z) \exp(b_m z')$ we find

$$\langle T_n^k(t) \rangle = k \sum_{m=2}^n m \int_t^\infty dt' f_{nm}(t, t') \langle T_m^{k-1}(t') \rangle. \quad (\text{A17})$$

This recursion yields Eq. (26).

APPENDIX B: Coefficients $d_{n;j_1,j_2}$ for $n = 2, \dots, 10$

In Tab. I we give the coefficients $d_{n;j_1,j_2}$ determining the second moment $\langle T_n^2 \rangle$ according to Eq. (27) for $n = 2, \dots, 10$. Note that the coefficient for $n = 2$ is consistent with Eq. (14).

j_2	j_1	2									
2	4	4									
j_2	j_1	2	3								
2	6	3									
j_2	j_1	2	3	4							
2	$\frac{36}{5}$	6	$\frac{6}{5}$								
4			$\frac{8}{5}$								
j_2	j_1	2	3	4	5						
2	8	$\frac{60}{7}$	3	$\frac{3}{7}$							
4			4	1							
j_2	j_1	2	3	4	5	6					
2	$\frac{60}{7}$	$\frac{75}{7}$	5	$\frac{9}{7}$	$\frac{1}{7}$						
4			$\frac{20}{3}$	3	$\frac{1}{3}$						
6					$\frac{2}{7}$						
j_2	j_1	2	3	4	5	6	7				
2	9	$\frac{25}{2}$	7	$\frac{27}{11}$	$\frac{1}{2}$	$\frac{1}{22}$					
4			$\frac{28}{3}$	$\frac{63}{11}$	$\frac{7}{6}$	$\frac{7}{66}$					
6					1	$\frac{1}{6}$					
j_2	j_1	2	3	4	5	6	7	8			
2	$\frac{28}{3}$	14	$\frac{98}{11}$	$\frac{42}{11}$	$\frac{14}{13}$	$\frac{2}{11}$	$\frac{2}{143}$				
4			$\frac{392}{33}$	$\frac{98}{11}$	$\frac{98}{39}$	$\frac{14}{33}$	$\frac{14}{429}$				
6					$\frac{28}{13}$	$\frac{2}{3}$	$\frac{2}{39}$				
8							$\frac{16}{429}$				
j_2	j_1	2	3	4	5	6	7	8	9		
2	$\frac{48}{5}$	$\frac{168}{11}$	$\frac{588}{55}$	$\frac{756}{143}$	$\frac{24}{13}$	$\frac{24}{55}$	$\frac{9}{143}$	$\frac{3}{715}$			
4			$\frac{784}{55}$	$\frac{1764}{143}$	$\frac{56}{13}$	$\frac{56}{55}$	$\frac{21}{143}$	$\frac{7}{715}$			
6					$\frac{48}{13}$	$\frac{8}{5}$	$\frac{3}{13}$	$\frac{1}{65}$			
8							$\frac{24}{143}$	$\frac{3}{143}$			
j_2	j_1	2	3	4	5	6	7	8	9	10	
2	$\frac{108}{11}$	$\frac{180}{11}$	$\frac{1764}{143}$	$\frac{972}{143}$	$\frac{36}{13}$	$\frac{9}{11}$	$\frac{405}{2431}$	$\frac{3}{143}$	$\frac{3}{2431}$		
4			$\frac{2352}{143}$	$\frac{2268}{143}$	$\frac{84}{13}$	$\frac{21}{11}$	$\frac{945}{2431}$	$\frac{7}{143}$	$\frac{7}{2431}$		
6					$\frac{72}{13}$	3	$\frac{135}{221}$	$\frac{1}{13}$	$\frac{1}{221}$		
8							$\frac{1080}{2431}$	$\frac{15}{143}$	$\frac{15}{2431}$		
10								$\frac{10}{2431}$	$\frac{10}{2431}$		

TABLE I Shows coefficients $d_{n;j_1,j_2}$ occurring in Eq. (27) for $n = 2, \dots, 10$. Coefficients for odd values of j_2 vanish.